Quantum cascade laser-based substance detection: approaching the quantum noise limit

Peter C. Kuffner[a], Kathryn J. Conroy[a], Toby K. Boyson[a], Greg Milford,[a] Mohamed A. Mabrok,[a] Abhijit G. Kallapur[a], Ian R. Petersen[a], Maria E. Calzada[b], Thomas G. Spence,[c] Kennith P. Kirkbride[d] and Charles C. Harb [a]

[a] School of Engineering and Information Technology, University College, The University of New South Wales, Canberra, ACT, 2600, Australia.
[b] Department of Mathematical Sciences, Loyola University New Orleans, New Orleans, LA, 70118, USA.
[c] Department of Chemistry, Loyola University New Orleans, New Orleans, LA, 70118, USA.
[d] Forensic and Data Centres, Australian Federal Police, Weston, ACT, 2611, Australia.

ABSTRACT

A consortium of researchers at University of New South Wales (UNSW@ADFA), and Loyola University New Orleans (LU NO), together with Australian government security agencies (e.g., Australian Federal Police), are working to develop highly sensitive laser-based forensic sensing strategies applicable to characteristic substances that pose chemical, biological and explosives (CBE) threats. We aim to optimise the potential of these strategies as high-throughput screening tools to detect prohibited and potentially hazardous substances such as those associated with explosives, narcotics and bio-agents.

Keywords: Quantum Cascade laser, Trace gas detection, Cavity Ringdown Spectroscopy, IR detection, Forensics

1. INTRODUCTION

Analysis of bulk organic explosives is a straightforward task for well-equipped forensic laboratories, but it is more difficult to analyse trace amounts of organic explosive residues (particularly in highly-contaminated post-blast samples); this usually requires an elaborate sequence of solvent extraction from swabs and some form of chromatographic or electrophoretic separation. Suitable detection techniques include ion mobility spectrometry (IMS), mass spectrometry and thermal energy analysis. However, such analytical systems lack the sensitivity to analyse explosive residues in vapour samples because of the very low vapour pressures characteristic of common organic explosives.

In this research, we aim to develop a cavity-enhanced spectroscopic instrument as a high-throughput screening tool for trace explosive detection, and potentially for other threats such as biological or chemical hazards. The method that will be used to achieve this aim is cavity ringdown spectroscopy (CRDS)[1,2] which is a laser-based direct-absorption technique. CRDS offers a significant increase in sensitivity, sufficient to permit detection of organic explosives in the vapour phase. This will provide a complementary technique for laboratory analysis of explosives, using vapour-phase samples rather than solvent extracts.

Figure 1 shows some of the main components that are required to successfully produce a laser based wide-band ($4\mu m$ to $12\mu m$), infrared spectrometer. Unlike an FTIR spectrometer, this laser-based system requires several features to construct a high resolution spectrum that at present are not commercially available. A laser will be required, instead of a thermal source, that can be frequency tuned over this vast wavelength range: as yet no single affordable source is available. A high finesse optical cell (cavity) that is vacuum compatible and a suitable photodetector will also be required. Although the optical coating technology does exist to make high Finesse cavities in this wavelength range, they cannot produce a single set of mirrors to cover the entire range.

Further author information: E-mail: c.harb@adfa.edu.au, Telephone: +61 2 6268 8203

The other important components include the Data Acquisition system (DAQ) to acquire the data; the control system and electronics to produce signals that can be used to adjust the system parameters; as well as the Digital to Analog converters and amplifiers to drive the system components such as the piezo electric transducers (PZTs). Additionally, clever data processing will be required to extract the information from the DAQ to produce an estimate for the cavity ringdown time τ, which can in turn be used to rapidly generate a spectrum, and consequently a determination of the absorbing species in the sample.

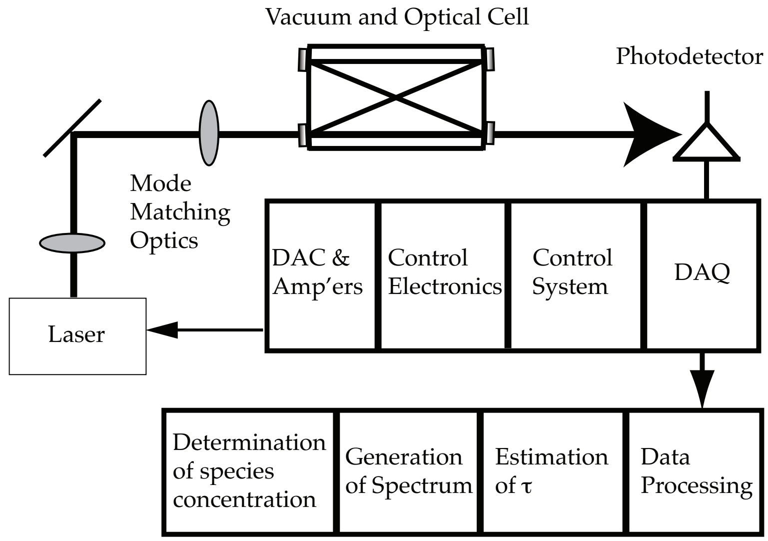

Figure 1. Components of a laser-based wide-band spectrometer.

In this paper, we will discuss our progress in developing such a spectrometer. In particular, we will discuss our use of commercially available components to build a test bed that we can use to apply new digital signal processing techniques that will ultimately allow us to construct a wide-band laser-based spectrometer in the molecular fingerprinting wavelength range (4μm to 12 μm). In this paper, we will discuss the system requirements and maximum signal to noise that could be achieved with our apparatus. This paper will discuss the characteristics of the quantum cascade laser (QCL) and Mercury Cadmium Telluride (MCT) detectors that we have available for this work; the progress on the CRDS system we are developing; and the digital signal processing techniques that we intend to employ to extract the absorption data.

In section 2 we will discuss the digital data rates that will be required to reach the maximum signal to noise of the system, which is set by the laser's quantum (or shot) noise. Section 3 will discuss the characteristics of the Quantum Cascade laser that we have available for this research. Section 4 discusses the characteristics of our CRDS system. This is followed, in section 5, by a discussion of the signal processing techniques that we are developing for this spectrometer.

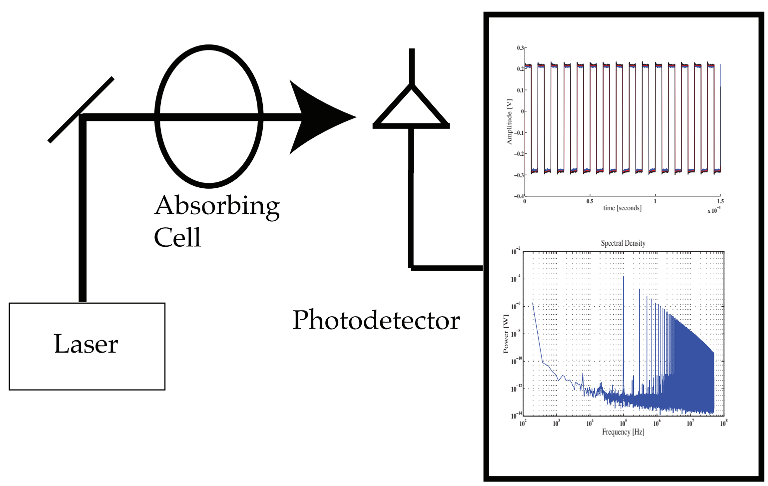

Figure 2. The simplest laser based absorption measurement setup. It consists of a scannable laser, a photodetector, a voltmeter and/or an radio frequency spectrum analyser.

2. DIGITAL DATA RATES REQUIRED

To determine the data rates that are required to record the signals from the simplified experiment shown in Fig. 2 we need to consider at minimum the photon noise statistics of the laser source and the photocurrent sampling rate. We shall ignore at this point the extra resources that maybe required for digital signal processing.

2.1 Quantum Noise Limit in the Infrared Region

Photons are bosons and hence they can all have the same wave-function. So the detection of the photons (from a laser or thermal source) is governed by the Poissonian statistics. Figure 2 shows the simplest laser based absorption measurement. It consists of a laser that is tunable in wavelength over the region of interest and a detector that is sensitive to the laser photons. The photo current produced by the detector is measured on an appropriate instrument such as a digital oscilloscope or a data acquisition system. The recorded voltage time series can be Fourier transformed to reveal the frequency domain spectrum of the measurement at every given laser wavelength.

To observe the maximum signal to noise ratio for this measurement, we would need a detection system that was limited by the quantum noise fluctuation of the laser. In our case, we will measure at absorption profiles at 6.1μm, the following calculation is reproduced to determine the digitizer resolution required to observe the mean photocurrent and the noise fluctuations simultaneously.

2.1.1 Data Rate required to reach Shot Noise Limited Sensitivity

The shot noise in a detector system is the noise due to the statistical variation in the arrival of photons in the incident light.

The average number of photons incident on the detector will be $\overline{n} = \Phi\tau$, for a given photon flux (Φ) and a known integration time interval (τ). The variance in the photon number will then be:

$$\sigma_n^2 = \overline{n^2} - \overline{n}^2 = \overline{n} = \Phi\tau \tag{1}$$

since the statistical distribution of the photon flux is Poissonian.[3] The average photocurrent is $\overline{I} = \Phi e$. The variance in the current will be:

$$\begin{aligned} \sigma_I^2 &= \overline{I^2} - \overline{I}^2 = \left(\frac{e}{\tau}\right)^2 \left(\overline{n^2} - \overline{n}^2\right) = \left(\frac{e}{\tau}\right)^2 \overline{n} \\ &= \frac{\overline{I}e}{\tau} \end{aligned} \tag{2}$$

From this we can determine the shot noise, since $i_{shot}^2 = \sigma_I^2$, $I = \overline{I}$, and $B = \frac{1}{2\tau}$. The shot noise current is then:

$$i_{shot} = \sqrt{\sigma_I^2} = \sqrt{\frac{eI}{\tau}} = \sqrt{2eIB} \tag{3}$$

The same derivation method applies to the voltage output from a detector, and it can be shown that the shot noise voltage is:

$$v_{shot} = \sqrt{2eVB} \tag{4}$$

To calculate the shot noise limit for an incident laser beam, the average current is given by the ideal photocurrent. This is the case when each photon striking the detector produces an electron-hole pair, so the photocurrent is $I = \frac{e\lambda P_o}{hc}$.

The noise spectral density for this case is then given by:

$$\frac{i_{shot}}{\sqrt{B}} = \sqrt{\frac{2e^2\lambda P_o}{hc}} \tag{5}$$

Figure 3 shows the number of bits that a data acquisition system would require to measure the mean photocurrent (the DC component) as well as the fluctuation due to shot noise (the AC component). The digitizer would need to measure a signal to noise ratio of 1.74×10^8 at 6.1μm which would require at least a 27 bit digitizer to record at the radio frequency of the AC fluctuation. At present 24 bit digitizers are available but only for the audio frequencies.

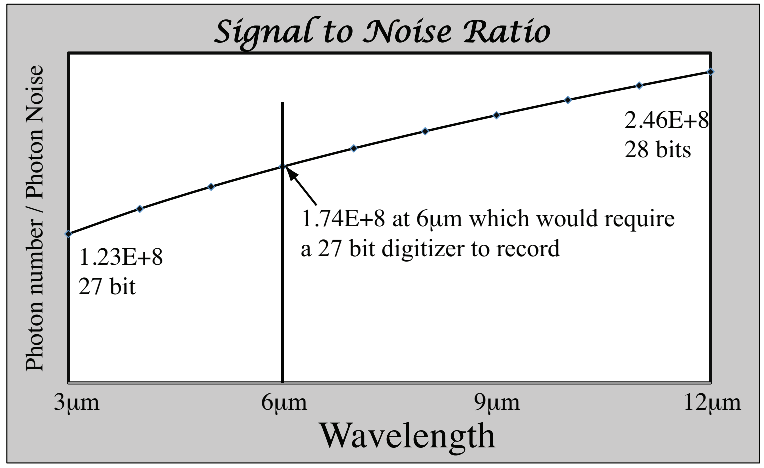

Figure 3. The signal to noise ratio for a 6μm 1 mW CW laser. In this case a 27 bit digitizer would be required to measure the DC and AC components simultaneously.

If we assume a spectral bandwidth comparable to that obtained from a commercial FTIR spectrometer operating in the 3μm to 12 μm wavelength range then we need to take a spectral measurement every 10MHz (3.3×10^{-4} wave numbers). If we further assume that we require a 10Hz spectrum update rate the we find that the data rate required $\approx$ 2Gbits/s with a clock frequency of 75MHz. With these conditions the sensitivity of the measurement would be:

$$S \approx \frac{1.74 \times 10^8}{\sqrt{75 \times 10^6}} \approx 2 \times 10^5 \tag{6}$$

which is 3 orders of magnitude better than standard FTIR spectrometers, but considerably more digital resources are required.

3. QUANTUM CASCADE LASER OPERATION

The quantum cascade laser (QCL) has been increasingly growing in its applicability to the spectroscopic absorption measurements, and is now recognised as an invaluable tool in this research area.[4–6] Although many articles have been written about the use of QCLs for spectroscopic detection there is still considerable developments required to see their deployment in general use. In this section, we will outline the characteristics of the QCL that we will use for this research and the limits we expect to reach.

3.1 Daylight Solutions MCT-2TE-100 Characterisation

The detectors we are using in the lab are two of Daylight Solutions' model HPC-2TE-100 detectors. These are 2-stage thermoelectrically (TEC) cooled, AC-coupled, photoconductive detectors, with the following parameters given with the datasheet.

The detector module consists of a photoconductive MCT detector: Vigo Systems Model # PCI-2TE-10.6-1x1-ZnSeW-HMS, with a pre-amplifier with 40dB gain. See Table 1 for further details. The power requirements for this module include a current draw of ≈90mA on the +15VDC rail and the ≈330mA on the +5VDC rail.

The detector parameters are listed in Table 2. The specific detectivity is given by the manufacturer for a bandwidth of 1Hz, normalised to an optical power of 1W, and a detector area of 1cm^2. The detectors have a detector area of 1mm×1mm square with a special ZnSe window fitted with a cutoff wavelength of $\approx 2\mu$m, and feature a hemispherical lens to give a wide angle of acceptance.

3.2 QCL Noise Characteristics

Figure 4 shows the noise as measured on an radio frequency spectrum analyser (Agilent E4411B spectrum analyser with an input impedance of 50Ω, at a resolution bandwidth of 30kHz) in both operation modes from a Daylight Solutions MCT detector.

A Daylight Solutions tunable mid-IR external cavity laser system - (Model TLS- 21XX Tuneable QCL Controller CW/Pulsed) was used in this investigation. In the CW case, the maximum power from the QCL in the lab is 25mW at 6.12μm. The measurement configuration used is as shown in Fig. 2. For this CW incident power from the QCL, the shot noise spectral density has a value of $1.98\times10^{-10}\mathrm{A}/\sqrt{Hz}$ as calculated from equation 5. This is well below the dark noise value shown in Fig. 4 (Top), and clearly there is no evidence of shot noise.

Figure 4 (Middle and Bottom) show the radio frequency noise and time trace characteristics of the same QCL. The top right trace shows the comb of frequencies associated with the 100kHz pulse rate. It also shows the excess noise that is present in the system when operating in pulsed mode. The >30dB increased noise level compared to the dark noise implies that the system has an excessive residual intensity noise. This is further confirmed by the time trace (bottom) that shows the pulse structure to be very irregular compared to the trigger pulse. We are working to determine the case of this excess noise.

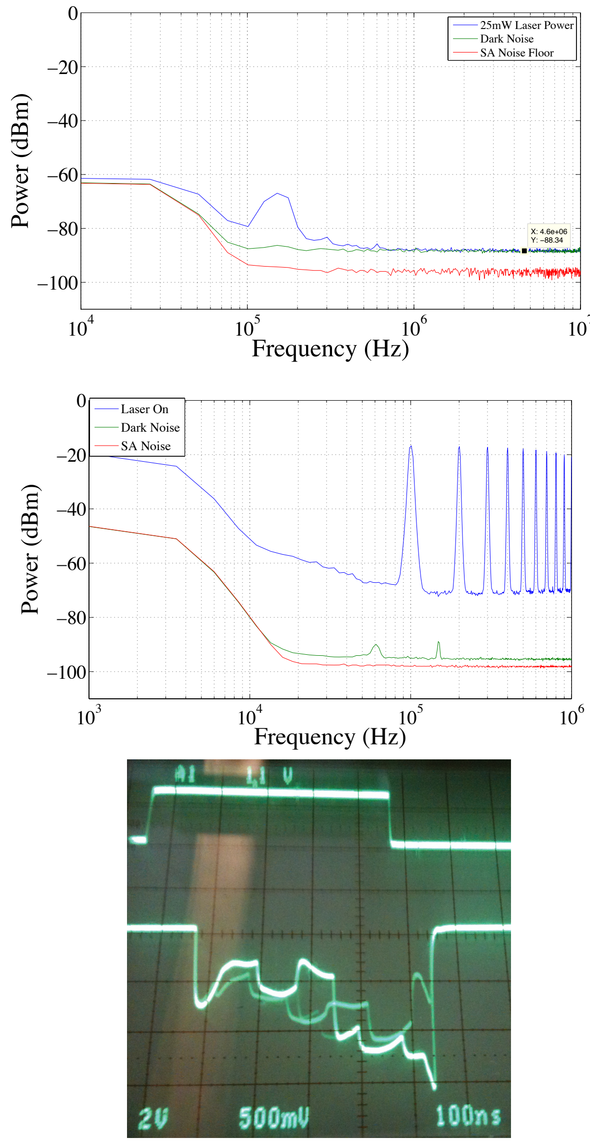

Figure 4. Top: Noise characteristics for 25mW of detected CW power, 30kHz RBW; Middle: Noise Characteristics for 1.86mW (in pulsed mode) 100kHz repetition rate, 500 ns pulse width 3KHz RBW; Bottom: oscilloscope trace showing the trigger pulse and the output signal.

3.3 QCL Beam Profile

Figure 5 show our QCL laser beam profile at 4 different locations along the beam path, and on both sides of a beam waist. The profiles were recorded on a Pyrocam from Ophir-Spiricon, LLC. As can be seen from the images the laser's shape is not a TEM_{00} mode. Also, the relative heights of the dominant features vary at different positions along the beam path. At this stage we are unsure if the beam from the laser is multimodal or the Pyrocam is not registering the profile correctly.

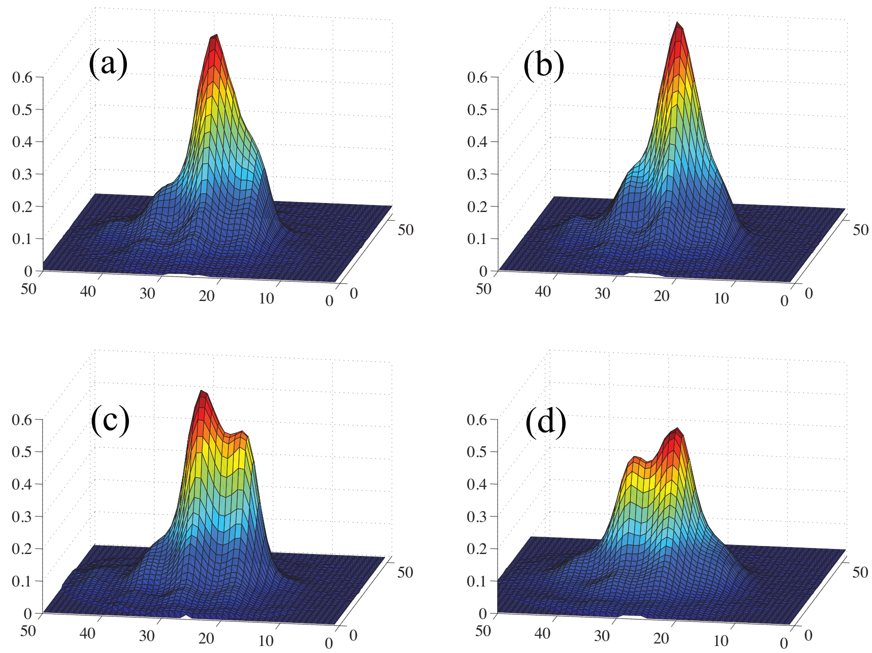

Figure 5. The QCL laser profile measured at 4 different positions along the beam path.

4. CRDS SYSTEM

4.1 Vacuum System and Cavity Parameters

The vacuum and optical cavity system, specially made for this research, is shown in Fig. 6. Here, we have designed the optical cavity to include a 4 mirror configuration in a ring shape. The mirrors are used as the vacuum seals, and are arranged such that an O-ring is sandwiched between the aluminum spacer and the mirrors. A backing plate, made also of aluminum, is used to hold the mirrors firmly in place. Two of the backing plates also house PZT elements that are used to adjust the cavity length as required. Each of the two PZTs are quoted to have a resonant frequency of 30KHz, a capacitance 180nF and a maximum stroke of 18 microns. This unit currently holds a vacuum of $\approx$ 0.2mbar.

The optical cavity consists of one input and one output mirror, that each have a reflectivity of 99.8 %, with unknown transmissivity and loss. The other two mirrors (the piezo driven units) are quoted to have a reflectivity of 99.995 %, also with an unknown transmissivity and loss. All 4 mirrors are are 1" diameter Plano/Concave with and ROC of 1m, and are made from a ZnSe substrate. The angle of incidence on each mirror is 2 degrees and the spacing between the mirrors is 0.5m, making a optical perimeter os $\approx$ 2m. We calculate the free spectral range to be 300MHz, and the beam waist within the cavity to be 918 μm.

In addition to the laser and optical cavity, a set of optics are used to mode match one to the other. Firstly, a wire grid polariser is placed in the beam path, just at the output apertature of the QCL and before the QCL's first external waist, located 110mm away. The polariser is used to control the output power and polarisation of the QCL. The QCL waist is placed 1.75m from the waist position inside the optical cavity. Using two plano-convex CaF2 lenses, mode matching of the QCL to the waist of the optical cavity is achieved with a 100mm focal length lens followed by a 250mm focal length lens.

4.2 Transfer Functions

In preparation for the possible development of laser sources that can cover this wavelength range we are designing a spectrometer to be quickly scannable. Figure 7 shows the transfer function of the high voltage amplifier (HV amp), PZT and mirror combination in the vacuum cell. The transfer function was recorded with a Agilent 10Hz

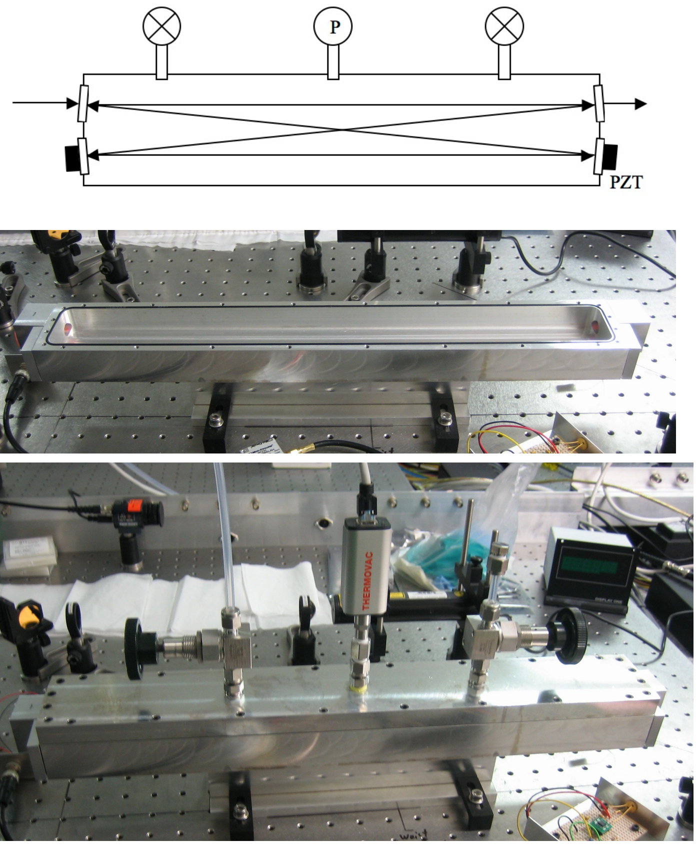

Figure 6. CRDS Vacuum system.

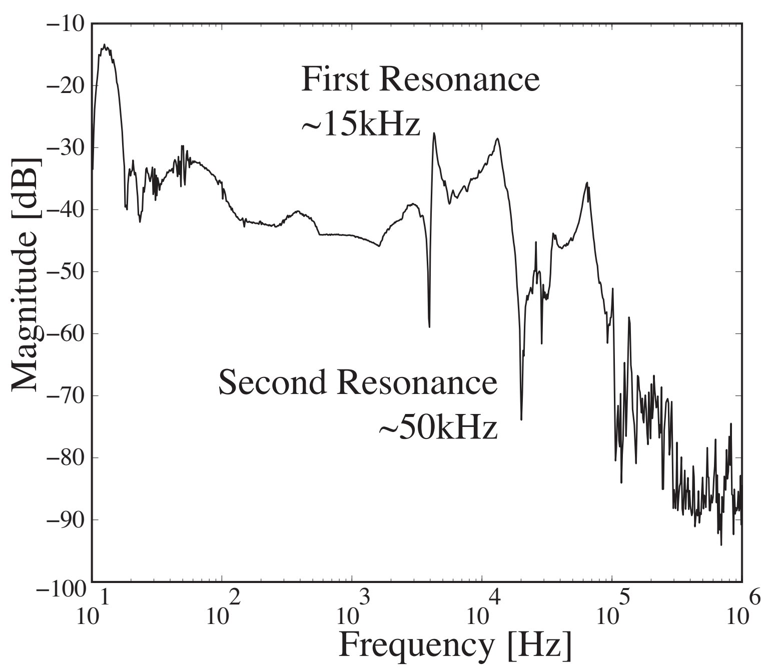

Figure 7. The transfer function for the high voltage amplifier (HV amp), PZT and mirror combination in the vacuum cell.

to 500MHz Network Analyser. Although the transfer function appears to be complicated only two features are important for the control loop. Resonances appearing at $\approx$ 15kHz and 50kHz will be used to to design a suitable controller.

The cavity will be held in lock with the input laser frequency using a PI controller. We will use techniques from modern control theory such as linear quadratic Gaussian (LQG) control[7,8] and other $H_2/H\infty$ control methods to improve locking in the presence of noise and uncertainties. These techniques are beyond the scope of this paper.

5. DIGITAL SIGNAL PROCESSING

5.1 Control Systems

Figure 1 shows the basic configuration for a laser-based wide-band spectrometer that could cover the same spectral wavelength region as a standard FTIR. The system requirements for the laser-based system are, however, fundamentally different. In this system, there are two types of control loops used to operate the system. The first is used to control the laser and cavity scan dynamics so that efficient cavity build up and ringdown can be achieved. This uses the transfer function discussed in section 4.2 to actively adjust the laser and cavity dynamics by a combination of feedback and feedforward methods.

The estimation channel is used to determine a value for the ringdown time τ as a function of wavelength, and hence the absorption spectrum. The following sections will outline some of these issues, and recent advances in solving the associated technical difficulties.

5.2 Data Rate Required to Measure τ to SNL Sensitivity

As discussed in Section 2.1, the data rate required to reach the QNL for a single-pass laser-based wide-band spectrometer with a spectral resolution similar to that obtained from a commercial FTIR spectrometer operating in the 3 to 12 μm wavelength range is $\approx$ 2.0Gbits/s. This is far less than what is required for a cavity enhanced spectrometer, such as a CRDS system, to reach the QNL. The benefit, however, of much better sensitivity greatly outweighs this disadvantage.

Commercially available CRDS systems typically have a limited number of wavelengths of operation. They also typically stay at one of the available wavelength for the measurement time, record the ringdowns and then fit the data using a fitting routine, such as a Levenberg-Marquardt (LM) algorithm, to make an estimate for τ. This data collection process limits the CRDS analysers to a few Hz of operation.

5.3 Real Time determination of τ

Considering the logarithm of the decay of the cavity field, conventional linear least square techniques can be used to estimate the value for τ; see e.g., OKeefe *et. al.*[9] and Xie *et. al.*[10] Indeed, such methods are susceptible to systems noise characteristics and instrument offsets as mentioned in Istratov *et. al.*[11] and Mazurenka *et. al.*,[12] and have been applied to the case of isolated ringdowns. On the other hand, nonlinear least square methods such as the Levenberg-Marquardt (LM) technique can effectively handle system noise but are known to limit the data throughput to below 10Hz as mentioned in Everest *et. al.*[13]

Considering these issues we proposed the use of a discrete-time extended Kalman filter (EKF) to estimate the value for τ in simulation in Kallapur *et. al.*[14] Furthermore, we also demonstrated the offline application of the EKF to estimate the value for τ for a set of experimentally obtained cavity ringdown data for a Fabry-Perot optical cavity in Kallapur *et. al.*[15] Here, it was noted that the EKF estimation results for τ converged to the neighborhood of its expected true value within nine ringdown cycles. Indeed, as mentioned in Kallapur *et. al.*,[15] the results can be improved by considering modeling uncertainties associated with the dynamics of the cavity and implementing robust estimation schemes. To this end, we have shown in simulation in Kallapur *et. al.*[16] that a discrete-time robust EKF can be used to estimate the value for τ in the presence of general modeling uncertainties in addition to exogenous noise sources. We are currently working on applying the EKF and the robust EKF methods to the estimation of τ for a Fabry-Perot optical cavity using real-time tools such as DSpace® and field programmable gate arrays (FPGA).

Recently we have also shown that real time processing of the data is possible, with high accuracy, using a frequency domain analysis. That method analysed the output of the spectrometer as a whole, rather than just analysing individual ringdown transients. Boyson *et. al.*[17] simulated the technique, comparing it to LM non-linear least squares fitting, and used a modelocked CRDS instrument for proof-of-principle tests. Boyson *et. al.*[17] present results that determining a value for τ 500 times faster than equivalent LM techniques. The technique used by Boyson *et. al.* is also suited to FPGA implementation as the CRDS waveform can be demodulated with its frequency components using a simple multiplication process.

We are currently using a pulsed-laser system to explore the use of this frequency-domain analysis to extract τ from noisy signals using off-the-shelf FPGA evaluation hardware and a tunable pulsed dye laser source. This system demonstrates data acquisition rates in excess of 50 kHz with precision comparable to using a Levenberg-Marquardt fitting algorithm if sufficient time is allowed for the slower fitting method.

6. CONCLUSIONS

We present a preliminary research into the characteristics of apparatus we will use for our quantum cascade laser-based substance detection system. We show that reaching the quantum noise limit will be a challenge due to the sensitivity of the detectors and laser sources, but we present new data processing techniques that can make ringdown time measurements more than 500 times faster than conventional techniques. In future research will develop the full system to test the control techniques in real time.

APPENDIX A. TABLES

Characteristics	**HPC-2TE-100**
Spectral response	4-12μm
Detectivity	$> 2.5 \times 10^9$cmHz$^{1/2}$/W
Active detector area	1mm×1mm
Response Time	< 3ns
Responsivity	> 2500V/W
Power supplies	15VDC & 5VDC
Power consumption	<3Watts
Field of view	78°

Table 1. Daylight Solutions HPC-2TE-100 detector characteristics.

Characteristics	**Units**	**PCI-2TE-10.6**
λ_{op}	nm	10.6
Detectivity (λ_{peak},20KHz)	cmHz$^{1/2}$/W	$> 3.5 \times 10^9$
Detectivity (λ_{op},20KHz)	cmHz$^{1/2}$/W	$> 1.4 \times 10^9$
Responsivity-Width product @λ_{op} 1×1mm	Vmm/W	> 15
Response Time	ns	< 10
1/f Corner Frequency	kHz	1 to 20
Bias Current-Width Ratio	mA/mm	5 to 20
Sheet resistivity	$\Omega/\Box$	50 to 150
Acceptance angle, F/#	mA/mm	36, 1.62

Table 2. Photoconductive detector characteristics.

ACKNOWLEDGMENTS

We would like to thank the Australian Federal Police, National Science Foundation (NSF Grant #: 0728285), The Louisiana Board of Regents and the Australian Research Council for their support of this research.

REFERENCES

[1] K.W.Busch and M.A.Busch, [*Cavity-Ringdown Spectroscopy An Ultratrace-Absorption Measurement Technique*], ACS Symp. Ser. 720, American Chemical Society, Washington, DC (1999).

[2] Berden, G., Peeters, R., and Meijer, G., "Cavity ring-down spectroscopy: experimental schemes and application," *International Reviews in Physical Chemistry* **19**, 565 (2000).

[3] Saleh, B. E. A. and Teich, M. C., [*Fundamentals of Photonics*], Wiley-Interscience, New Jersey (2007 (2 edition)).

[4] Paldus, B. A., Harb, C. C., Spence, T. G., Zare, R. N., Gmachl, C., Capasso, F., Sivco, D. L., Baillargeon, J. N., Hutchinson, A. L., and Cho, A. Y., "Cavity ringdown spectroscopy using mid-infrared quantum-cascade lasers," *Optics Letters* **25(9)**, 666–668 (2000).

[5] Curl, R. F., Capasso, F., Gmachl, C., Kosterev, A. A., McManus, B., Lewicki, R., Pusharsky, M., Wysocki, G., and Tittel, F. K., "Quantum cascade lasers in chemical physics," *Chemical Physics Letters* **487**, 1–18 (2010).

[6] Capasso, F., "High-performance midinfrared quantum cascade lasers," *Optical Engineering* **49(11)**, 111102 (2010).

[7] Sayed Hassen, S. Z., Heurs, M., Huntington, E. H., Petersen, I. R., and James, M. R., "Frequency locking of an optical cavity using linear-quadratic gaussian integral control," *J. Physics B: At. Mol. Opt. Phys.* **42** (2009).

[8] Sayed Hassen, S. Z. and Petersen, I. R., "A time-varying Kalman filter approach to integral LQG frequency locking of an optical cavity," in [*American Control Conference*], (July 2010).

[9] O'Keefe, A. and Deacon, D. A. G., "Cavity Ring-Down Optical Spectrometer for Absorption Measurements using Pulsed Laser Sources," *Review of Scientific Instruments* **59**, 2544–2551 (Dec. 1988).

[10] Xie, J., Paldus, B. A., Wahl, E. H., Martin, J., Owano, T. G., Kruger, C. H., Harris, J. S., and Zare, R. N., "Near-Infrared Cavity Ringdown Spectroscopy of Water Vapor in an Atmospheric Flame," *Chemical Physics Letters* **284**, 387–395 (Mar. 1998).

[11] Istratov, A. A. and Vyvenko, O. F., "Exponential analysis in physical phenomena," *Rev. Sci. Instrum.* **70**(2) (1999).

[12] Mazurenka, M., Wada, R., Shillings, A. J. L., Butler, T. J. A., Beames, J. M., and Orr-Ewing, A. J., "Fast fourier transform analysis in cavity ring-down spectroscopy: application to an optical detector for atmospheric NO2," *Applies Physics B: Lasers and Optics* **81**(1), 135–141 (2005).

[13] Everest, M. A. and Atkinson, D. B., "Discrete Sums for the Rapid Determination of Exponential Decay Constants," *Review of Scientific Instruments* **79**, 023108–023108–9 (Feb. 2008).

[14] Kallapur, A. G., Petersen, I. R., Boyson, T. K., and Harb, C. C., "Nonlinear Estimation of a Fabry-Perot Optical Cavity for Cavity Ring-Down Spectroscopy," in [*IEEE International Conference on Control Applications (CCA)*], 298–303 (Sept. 2010).

[15] Kallapur, A. G., Boyson, T. K., Petersen, I. R., and Harb, C. C., "Nonlinear estimation of ring-down time for a fabry-perot optical cavity," *Opt. Express* **19**, 6377–6386 (Mar 2011).

[16] Kallapur, A. G., Petersen, I. R., Boyson, T. K., and Harb, C. C., "Robust nonlinear estimation for a fabry-perot optical cavity," in [*8th Asian Control Conference (to be presented)*], (May 2011).

[17] Boyson, T. K., Spence, T. G., Calzada, M. E., and Harb, C. C., "A frequency domain analysis method for cavity ring-down spectroscopy," *Optics Express* (2011). Excepted for Publication March 2011.